Thermal oxidation of vinyl ester and unsaturated polyester resins

Juan Sebastian Arrieta [a, b], Emmanuel Richaud [a, *], Bruno Fayolle [a], Fidèle Nizeyimana [b]

[a] PIMM, Arts et Métiers ParisTech, CNRS, 151 Bvd de l'Hôpital, 75013 Paris, France
[b] AREVA TN, 1 rue des hérons, 78180 Montigny-le-Bretonneux, France

A B S T R A C T

The thermal oxidative ageing of vinyl ester and unsaturated polyester was studied at temperatures ranging from 120 to 160 °C and oxygen pressures ranging from 0.02 to 2.0 MPa. The oxidation of both materials was shown to generate anhydrides detected by FTIR spectroscopy, the origin of which being the oxidation of CH_2 group in α position of ester, and significant mass loss. According to FTIR study, vinyl ester was shown to be more oxidizable than unsaturated polyesters but this feature is counterbalanced by a lower volatile yield. The thickness of oxidized layer in diffusion limited oxidation regime was hence observed to be higher in Unsaturated Polyester (ca 600 μm) than in Vinyl Ester (ca 200 μm) at 160 °C and seems not affected by the presence of high content of fillers.

Keywords:
Vinyl ester
Unsaturated polyester
Thermal oxidation
Gravimetry
InfraRed spectroscopy
Diffusion limited oxidation

1. Introduction

Unsaturated Polyester (UP) and Vinyl Ester (VE) thermosetting resins are two very common matrices for glass fibers reinforced composites in particular because of their low price and easy processing. The relatively viscous prepolymers are usually dissolved into styrene being both a solvent and a crosslinking agent. Then, adding an organic peroxide (often combined with a carboxylate salt used as accelerator) initiates the random copolymerization of styrene and prepolymer double bonds so as to get a crosslinked network.

UP and VE based materials can be envisaged as neutron shielding material for transport/storage casks of radioactive materials. Their shielding ability for neutron radiations comes from hydrogen atoms slowing down neutrons. Those properties are usually improved by adding high percentages of zinc borate, since boron atoms absorb neutrons and alumina trihydrate which is also a flame retardant [1]. However, in service conditions, thermosetting resins are submitted to enhanced temperatures (up to 160 °C) where the material can degrade.

The degradation of such materials was addressed in the case of water (see for example [2]) and photochemical ageing (see for example [3–7] for UP and [8,9] for VE), which covers the classical use conditions of UP and VE composites, or in the case of non isothermal degradation at temperatures where the direct thermolysis of the polymer is the main cause of degradation [10,11]. The conclusions of those works cannot be easily adapted to the case of thermal oxidative ageing at moderate temperatures, for which published data are scarce but suggest that oxidation would induce a significant mass loss [9]. This loss of volatile compounds might result in the decrease of the resin's shielding properties in the case of the transport of radioactive materials. Predicting the long term behavior of UP and VE submitted to thermal oxidative ageing requires at least understanding several issues addressed in this paper:

- The nature of the degradation mechanism since several sites are likely to undergo radical attack according to literature [3,9].
- The effect of temperature on oxidation kinetics since material will be subjected at temperatures continuously decreasing from the time at which radioactive materials are put into the container.

* Corresponding author.
E-mail address: emmanuel.richaud@ensam.eu (E. Richaud).

- The profile of degradation within the thickness of sample and the effect of oxygen concentration on the overall oxidation kinetics since the oxidation is limited by oxygen diffusion.
- The role of fillers in the oxidative process, being used in relatively high volume fraction in UP and VE resins. On one hand, fillers can interact with chemical mechanism involved in oxidation and on the other hand, they could modify oxygen diffusion in the diffusion limited oxidation regime and then change the oxidized layer depth for a given exposure condition.

This paper will hence present a study of VE and UP thin film oxidation studied by FTIR to investigate a part of the degradation mechanism. Corresponding kinetic curves of carbonyl generation and weight loss will be used for comparing their intrinsic oxidative stability and the subsequent changes in their shielding performances. Last, a comparison of thin and thick samples (unfilled or not) will allow the issue of control by Oxygen Diffusion to be addressed.

2. Experimental

2.1. Materials

UP was obtained from the condensation of a mixture of 1,2 propanediol + fumaric acid used as prepolymer (Fig. 1a) and 28% by weight of styrene. Based on FTIR titration of terminal OH group, its average molar mass was estimated ca 850 g mol^{-1}.

In VE, the prepolymer is composed of Bisphenol A Vinyl Ester (Fig. 1b) and Novolac (Fig. 1c) with weight ratio 1:3 with 33% by weight of styrene. Polymerization degree for Bisphenol A VinylEster and Novolac are respectively 0.15 and 2.6 (i.e. molar mass equal to 556 and 882 g mol^{-1}).

Materials were cured with an organic peroxide as initiator and a cobalt(II) carboxylate as catalyzer so as to obtain 70 μm average thickness films and plates with a 0.2–5 mm thickness. Both UP and VE were cured according the same classical conditions: 1 h gelation at room temperature followed by an isotherm (12 h at 80 °C). NB: some details are here missing for non-disclosure reasons but the resins under investigation are close to very common commercial systems for which manufacturers usually give information (nature and quantity of initiator and cycle cure).

Mineral fillers (alumina trihydrate and zinc borate) were mixed with the prepolymer/styrene up to 68% in mass proportion prior to cure. Their properties are recalled in Ref. [1].

2.2. Characterization

2.2.1. Exposure conditions

Samples were aged under atmospheric pressure in ventilated ovens thermostated at 120, 140 and 160 °C.

Some comparisons were done with exposures under enhanced oxygen pressure (up to 2.0 MPa) using a 1410 Top Industries Autoclave.

2.2.2. Fourier transform InfraRed

FTIR tests were performed on free standing films in transmission mode (4 cm^{-1}, 16 scans) using a Frontier spectrometer (Perkin Elmer).

2.2.3. Gravimetry

Samples aged in oven or autoclaves were regularly weighted during their thermal ageing using a Mettler Toledo XS105 balance.

Some samples were also aged *in situ* in the TGA cell using a Q50 TGA driven by Q Series Explorer (TA Instruments) so as to monitor continuously the mass loss of samples aged under inert (100% N_2) or pure oxidative atmosphere (100% O_2).

2.2.4. Optical microscopy

Oxidized thick samples were embedded into an epoxy-amine resin (Presi Mécaprex KM-V two stages resin) which was cured at room temperature. After obtaining a smooth and mirror like finish by polishing the samples, a Zeiss Axio Imager A2M optical microscope was used to measure the thickness of oxidized layer.

2.2.5. Oxygen permeability measurements

The oxygen transport properties of the materials were measured from the permeation kinetics of pure dioxygen (100% O_2) on rectangular samples cut from UP, VE and their composites. The permeability, diffusivity and solubility coefficients were determined from tests performed isothermally at 25 °C and 100 °C (the

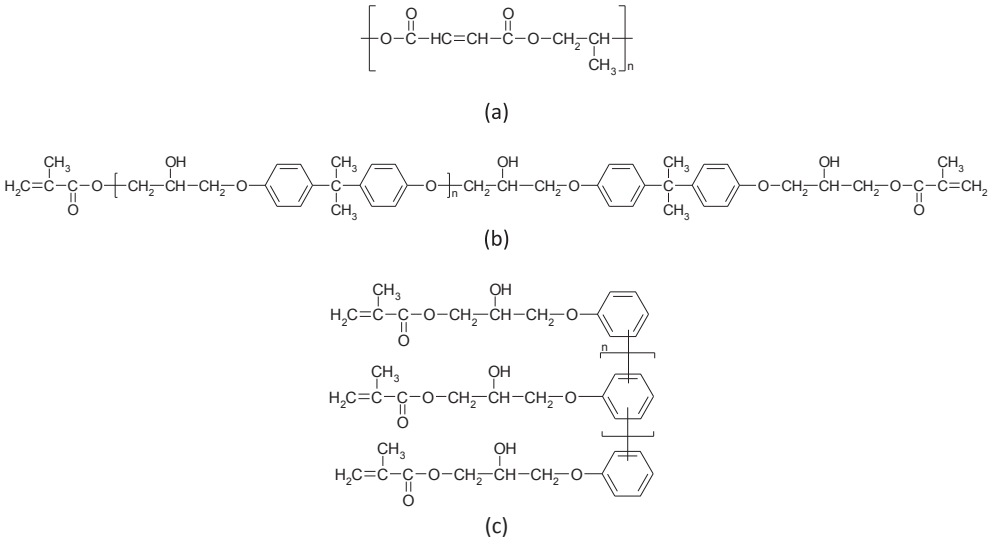

Fig. 1. Structure of prepolymers for Unsaturated Polyester (a) and Vinyl Ester (b and c).

experimental details are given in Ref. [12]).

3. Results

3.1. Oxygen permeability measurements

Oxygen permeability tests were performed on unfilled and filled VE and UP samples. Table 2 reports the oxygen permeability (P_{O2}) and diffusion coefficient (D_{O2}). Those data can be commented as follows:

- The apparent activation energies for diffusivity and permeability are given in Table 1. They are on the order of 20–30 kJ mol^{-1}, which is the expected order of magnitude for thermosets [13–15].
- Solubility coefficients (being the ratio of permeability over diffusivity) display no significant temperature changes since activation energies on permeability and diffusivity are very close.
- It seems that, within the experimental incertitude, filler has only a negligible effect on the diffusivity value.
- Last, the extrapolation of data suggests that oxygen diffusion coefficients in UP and VE are almost very close at 160 °C.

3.2. Comparison of samples with different thicknesses and study of diffusion limited oxidation

Oxidized thick samples were observed by optical microscopy. Their edges are noticeably darker than bulk (Fig. 2) which is ascribed to the presence of superficial degradation. It is observed that:

- The thickness of degraded layer seems to be very close for unfilled resins and their filled analogues.
- The thickness of degraded layer is lower for VE than UP.

We tentatively tried to confirm that this degraded layer was induced by the so-called Diffusion Limited Oxidation effects. For that purpose, we compared the weight loss curves for materials with various thicknesses aged under air (see Fig. 3). Let's note that the curves for filled materials were corrected by a term $1/(1-w_{filler})$ expressing the presence mineral filler (in weigh fraction w_{filler}) being almost inert under the exposure conditions under investigations.

Curves have some common features with epoxy-diamine networks for example [14–17] i.e. the absence of induction period, and the absence of any mass increase in the early exposure time but rather an instantaneous decrease (contrarily to PP for example [18]). Two regimes can be distinguished:

- The first one is characterized by a maximal mass loss rate. As it will be seen later, samples exposed under nitrogen also display a non-negligible mass loss in the same time range. It suggests that volatile compounds lost during this first stage are in part unreacted styrene, residues of polymerization initiator, adsorbed water… It seems also that mass loss is higher for filled than for unfilled samples, which suggests that fillers also display a slight thermal decomposition.
- The second one is assumed to describe the intrinsic thermal stability of materials. The assessment of the mass loss rate in this second regime suggests that there is obviously no effect of fillers on the spatial heterogeneity of degradation, consistently with the observations on diffusion coefficient value for filled and unfilled materials at 160 °C (see Table 2). A stationary rate was determined (see Fig. 3 for UP) and plotted versus reciprocal thickness (Fig. 4). Curves display the expected shape (Fig. 4): the degradation rate increases almost linearly at low reciprocal thickness and reaches a maximum at high reciprocal thickness corresponding to non DLO regime. More details and interpretations associated to this approach can be found elsewhere in the references [14–17]).

Since we lacked samples for covering all the 1/thickness range from 0 to 15 mm^{-1}, we have here estimated the thickness of oxidized layer as the intersect between the linear regression of high thickness data (left wing of the curve in Fig. 4) and the asymptote corresponding to the data for the thinnest sample (right wing of the curve in Fig. 4). This intersect is expected to correspond to the thickness above which oxidation is heterogeneous with concentration of oxidation products displaying a characteristic “U shape”. Its value is equal to twice the Thickness of Oxidized Layer (TOL).

According to this graphical method, the TOL would be ca 65 μm for VE and 125 μm for UP. Despite the uncertainty linked to the method for determination, it seems clear that the degraded layer is actually 2 times sharper for VE than for UP (as suggested by microscopy and the

Table 1
Oxygen permeability (P_{O2}) and oxygen diffusion coefficients (D_{O2}) for non-oxidized unfilled and filled VE's and UP's samples together with the estimation of the activation energies for each material. Values at 160 °C correspond to an extrapolation of values at 25 and 100 °C.

	Temperature (°C)	P_{O2} (m^3(STP) m^{-1} Pa^{-1})	D_{O2} (m^2 s^{-1})
VE unfilled	160	21×10^{-18}	28.8×10^{-12}
	100	7.5×10^{-18}	7.7×10^{-12}
	25	1.2×10^{-18}	0.7×10^{-12}
E_0 (kJ mol^{-1})	–	22.6	29.5
VE filled	160	102.3×10^{-18}	24.1×10^{-12}
	100	14.9×10^{-18}	7.5×10^{-12}
	25	0.2×10^{-18}	0.9×10^{-12}
E_0 (kJ mol^{-1})	–	43.1	26.1
UP unfilled	160	47.0×10^{-18}	49.4×10^{-12}
	100	23.4×10^{-18}	19.5×10^{-12}
	25	6.6×10^{-18}	3.6×10^{-12}
E_0 (kJ mol^{-1})	–	15.6	20.8
UP filled	160	74.9×10^{-18}	34.9×10^{-12}
	100	23.6×10^{-18}	13.3×10^{-12}
	25	2.9×10^{-18}	2.3×10^{-12}
E_0 (kJ mol^{-1})	–	25.8	21.6

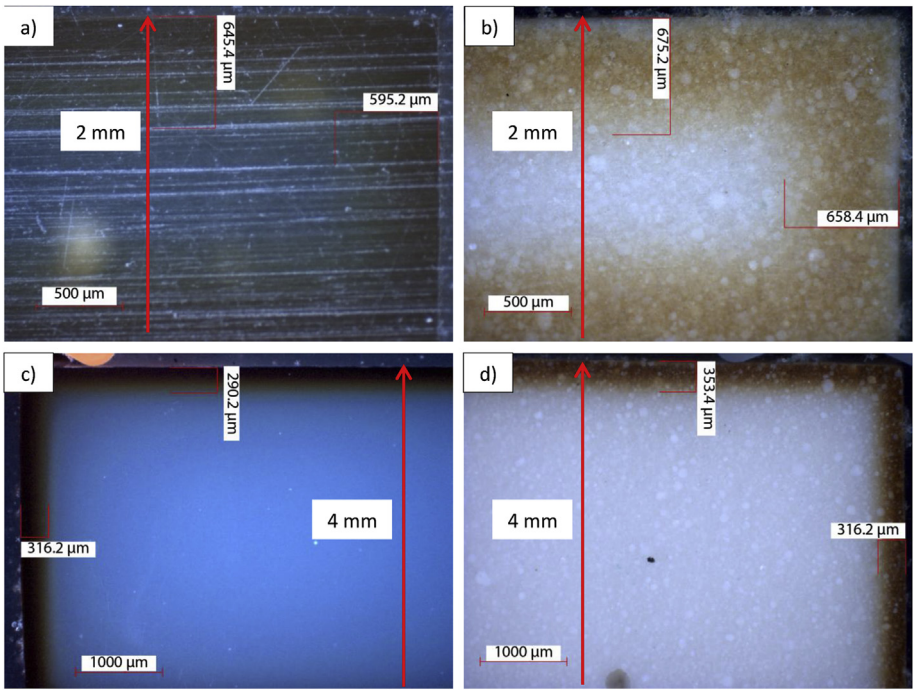

Fig. 2. Oxidized layer thickness measured by optical microscopy of UP (a: unfilled, b: filled) and VE (c: unfilled, d: filled) samples submitted to thermal ageing at 160 °C under atmospheric air during 700 h.

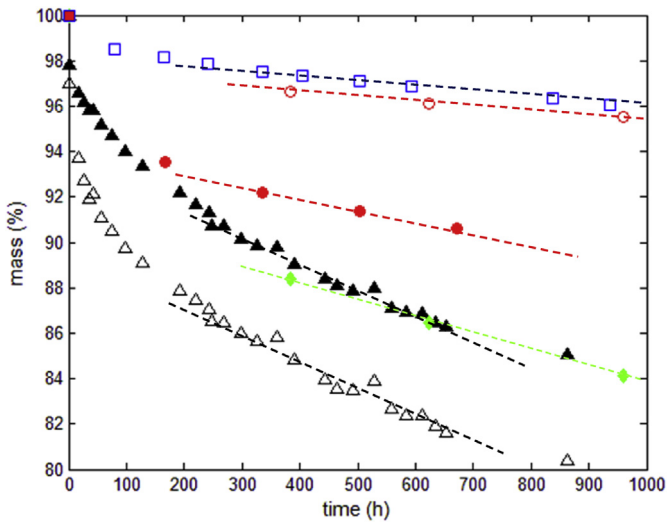

Fig. 3. Typical mass loss curves of UP for 200 µm (▲,△), 1 mm filled (◆), 2 mm (●,○), 5 mm (□) aged under air at 160 °C. Open and closed symbols correspond respectively to unfilled and filled materials. The dashed lines correspond to the "stationary regime" where the mass loss rates were determined (see text).

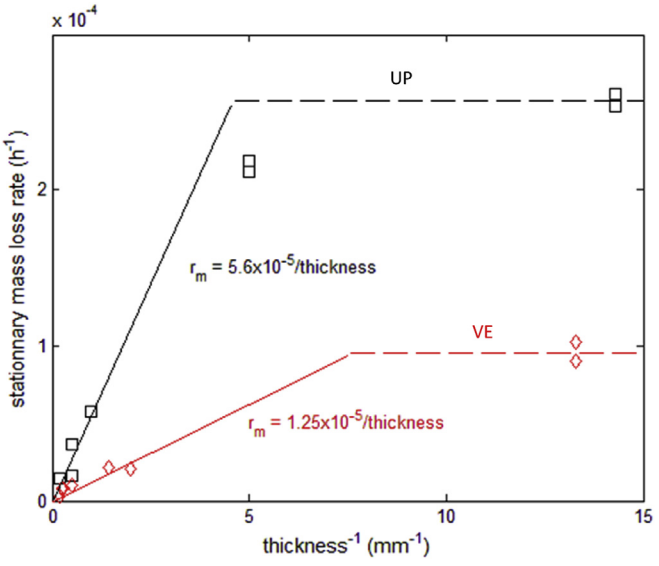

Fig. 4. Oxidation rate in function of the reciprocal thickness for samples of VE and UP and their composites submitted to a thermal degradation at 160 °C under atmospheric air.

estimation in Fig. 4) and that oxidation of 70 µm thin samples (used in the following) is not controlled by oxygen diffusion for both kind of materials.

3.3. Stable oxidation products

The FTIR spectra of virgin and aged Unsaturated Polyester (UP) and VinylEster (VE) 70 µm thin films (non DLO regime) are presented in Fig. 5. They display the main absorption bands at 3500 cm^{-1} (elongation of chain ends OH groups for UP and isopropanol group in VE), 3100–2850 cm^{-1} (elongation of aromatic and aliphatic C–H bonds), 1730 cm^{-1} (ester) and a broad absorbance in the fingerprint region due to C–O groups. The spectra of virgin samples and the assignment of all absorption bands are given in Appendix.

In order to better understand the nature of the reactive sites involved in thermal oxidation processes, some comparisons were done with:

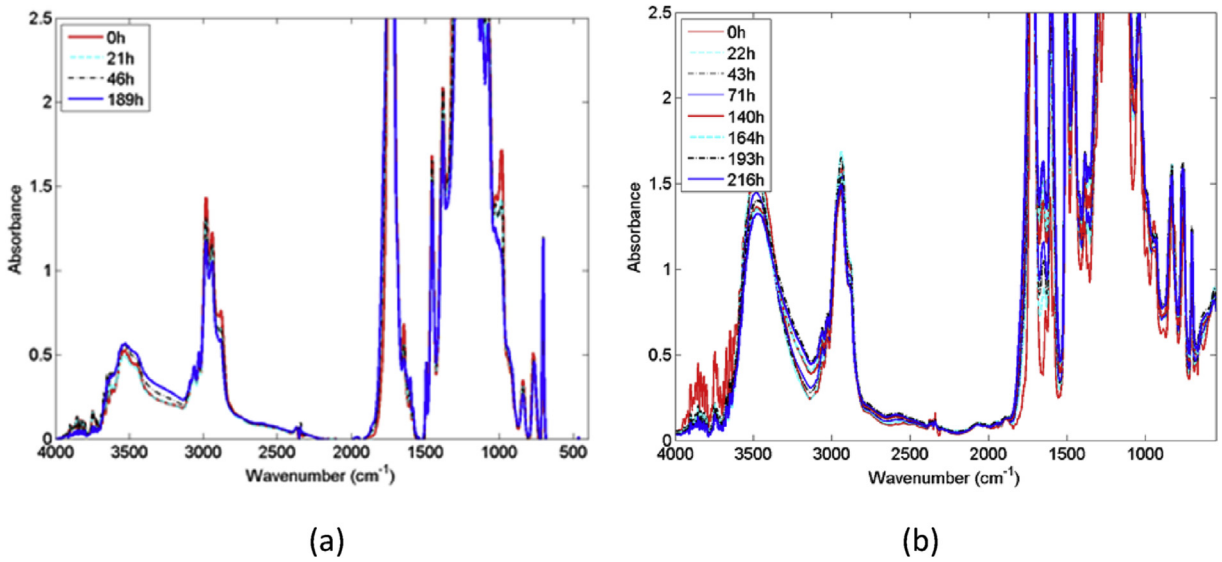

Fig. 5. FTIR spectra of virgin and oxidized UP and VE 70 μm films aged at 160 °C under atmospheric air.

- a bulk polystyrene synthetized by radical polymerization,
- materials similar to VE and UP but in which styrene was first evaporated under vacuum prior to polymerization (representing a 100% based prepolymer material) and aged directly on the KBr plates used for FTIR analysis.

Fig. 6 displays changes in carbonyl region for UP and its prepolymer (Fig. 6a and b), VE and its prepolymer (Fig. 6c and d) and in the hydroxyl and C—O region for VE (Fig. 6e and f).

Interpretation of FTIR spectra is tricky because of the strong absorption due to ester groups hold by prepolymer. However, it seems clear for us that:

- there is no evidence of carbonyl products generated by styrenic unit oxidation such as benzophenones at 1690 cm^{-1} [19].
- there is a certain similarity between the oxidation products in UP and in the material made from its prepolymer: both spectra mainly display only very minor changes apart the appearance of a shoulder at 1775 cm^{-1}. This signal is characteristic of the conversion of an ester into an anhydride [20].
- the spectra of VE and the material made from its prepolymer also display a wide shoulder centered at 1775 cm^{-1} identically to UP and its prepolymer. Moreover, a doublet appears in the C=C double bonds region (1650 and 1600 cm^{-1}). Last, a decrease of the signal at 1045 cm^{-1} (due to alcohol group) is witnessed.

An interpretation will be proposed in the "Discussion" section.

3.4. Kinetics of mass loss and carbonyl accumulation

In order to confirm that the mass loss in the second regime is associated to oxidation kinetics, mass loss and carbonyl formation were monitored for exposures under several temperatures and oxygen pressures.

Absorbances of the carbonyl regions were converted into concentrations and plotted versus time. Fig. 7 displays the comparison of thin UP and VE 70 μm thin films exposed under several conditions. First, it appears that irrespectively of the exposure conditions, the rate of carbonyl formation is higher for VE than for UP. This observation will be discussed later. Secondly, it is observed that an increase of oxygen pressure induces an increase of the rate of carbonyl formation (*i.e.* oxidation kinetics) for a given temperature, which was expected according to literature [21,22].

The weight variation of the materials was followed as function of time for UP and VE 70 μm films. Fig. 8 shows the comparison of UP and VE curves under N_2 or O_2 and Fig. 9 illustrates the effect of oxygen pressure on samples aged at 160 °C. The mass loss curves display two main phases:

- The first one is observed under air and under nitrogen. The most reasonable explanation is that it corresponds to the loss of the volatile residual reactants and initiator by-products.
- The second one is shown to be controlled by oxygen pressure and sample thickness, which corresponds to the loss of volatile compounds generated by oxidation (see also Fig. 9a).

According to Fig. 8 and 9, it seems that kinetics of mass loss in VE based materials is here slower than in UP materials. This apparent contradiction with FTIR results (Fig. 7) will be commented in the "Discussion" section. The effect of increasing oxygen pressure on mass loss kinetics was also illustrated in Fig. 9a. Fig. 9b shows curves of oxidation rate versus oxygen pressure. These curves display the classical hyperbolic shape [21,22]: oxidation rate linearly increases in the low oxygen pressure domain and plateaus under high oxygen pressures. On both UP and VE, the boundary between the two domains is $(P_{O2})_C \sim 0.2$ MPa.

This investigation was completed by comparing the effect of temperature on samples differing by their thickness under several different oxygen pressures (see Fig. 10 for Vinyl Ester and Fig. 11 for UP).

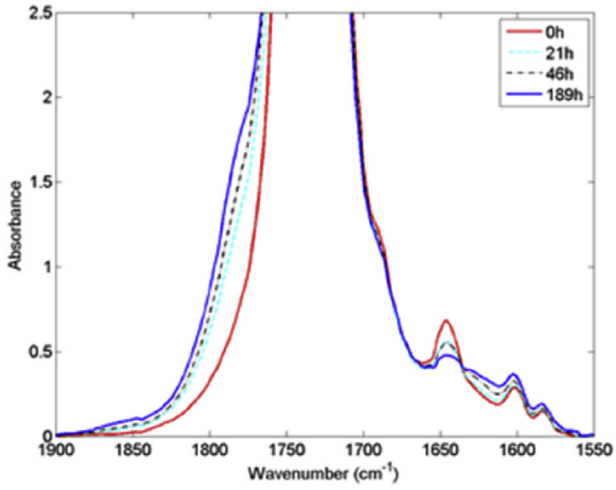

(a)

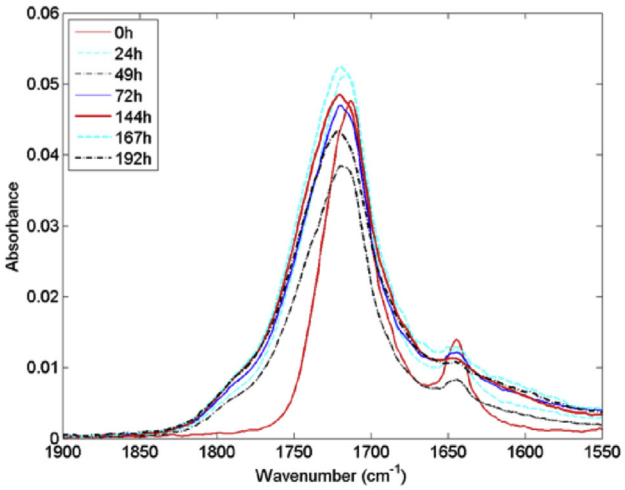

(b)

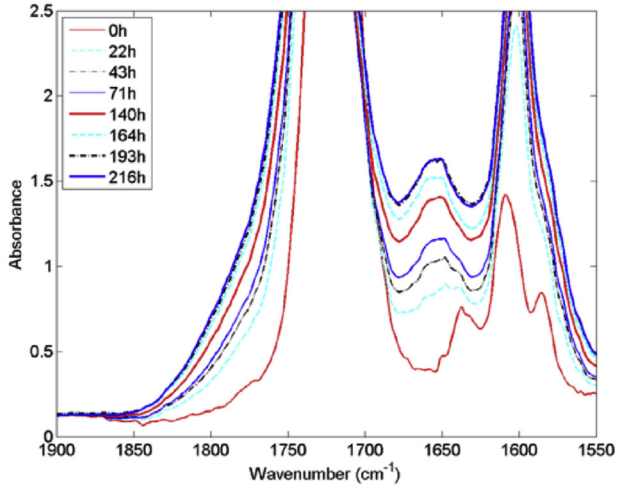

(c)

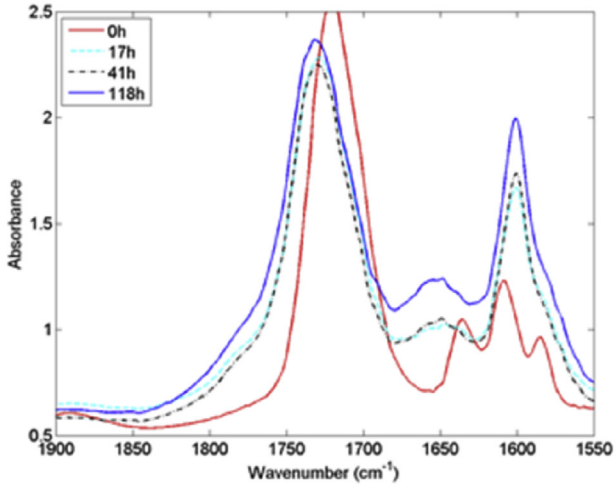

(d)

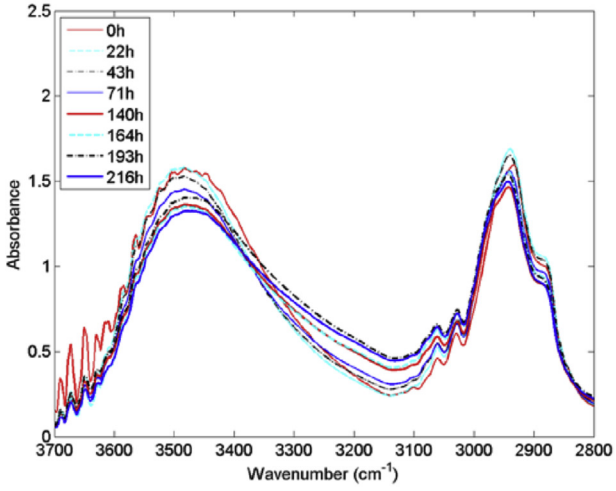

(e)

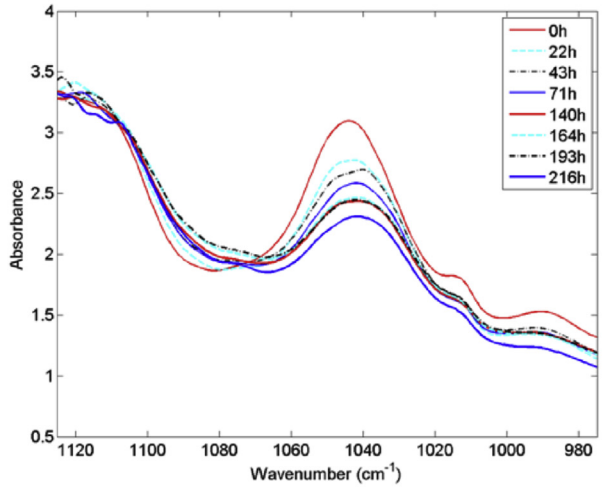

(f)

Fig. 6. FTIR spectra of Unsaturated Polyester (a) and its prepolymer (b), of Vinyl Ester (c,e,f) and its prepolymer (d).

Activation energies for mass loss and carbonyl build up range between two limits:

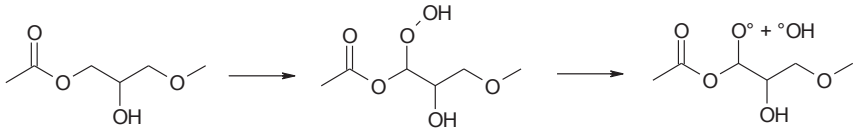

- for UP: from ca 50 kJ mol^{-1} for very thick samples (*i.e.* much more than the Thickness of Oxidized Layer) aged under air to ca 100 kJ mol^{-1} for thin films (*i.e.* lower than the Thickness of Oxidized Layer) under total oxygen excess.
- for VE: from 70 kJ mol^{-1} for very thick samples to ca 90 kJ mol^{-1} for thin films under total oxygen excess.
- samples having whether an intermediary thickness or aged under intermediary oxygen pressure fall in between.

4. Discussion

4.1. On the nature of oxidation products

For both UP and VE, the main change in FTIR spectra is the appearance of a wide shoulder at 1775–1800 cm^{-1}. According to literature, this indicates the formation of an anhydride coming from the oxidation of CH_2 in α position of ester group as observed in PLA [19] or in PET and PBT [23].

In UP, anhydride formation can be explained by the following simplified mechanism where C–H group generates alkoxy which reacts by β scission or cage process (in the case of secondary C–H):

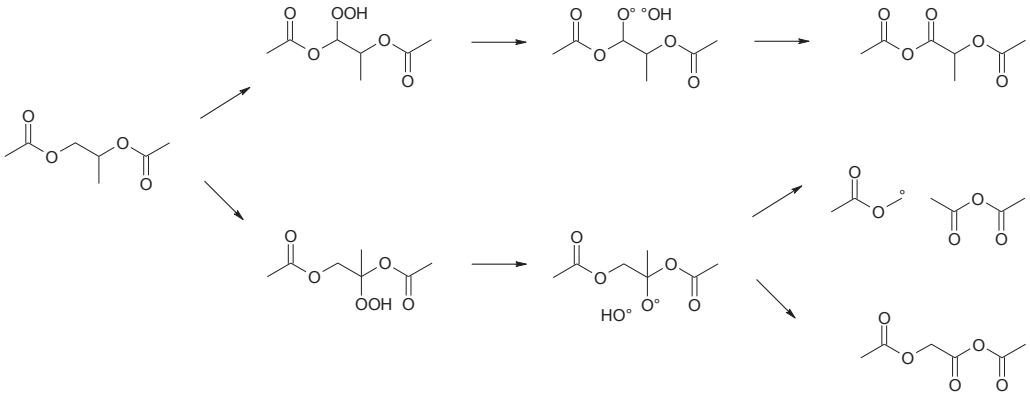

In VE, there are at least three sorts of reactive C–H located in α-position of oxygen atoms.

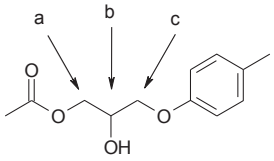

According to the existing literature on epoxies, C–H (c) will generate a phenyl formate (1730 cm^{-1}) and C–H (b) a carboxylic acid [24]. It is particularly intricate to conclude on the reactivity of both sorts of C–H group given the wide absorbance of ester groups belonging to virgin polymer in this region. In the case of C–H (a), oxidation will also generate a hydroperoxide:

The alkoxyl radical can react by several processes. The "in cage" reaction with another radical is actually expected to give an anhydride:

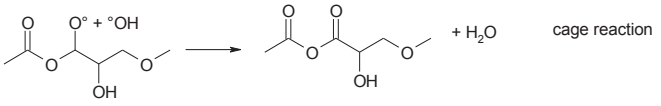

Oxidation in Vinyl Ester is also characterized by the appearance of a signal between 1600 and 1650 cm^{-1}. Such a signal was observed in the case of a Vinyl Ester aged at room temperature but not in the case of a Vinyl Ester resin aged at 140 °C [9]. Absorbances in this region of the FTIR spectra are usually attributed to double bonds as illustrated for example in the case of *N*-butyl vinyl ether displaying a doublet at 1640 and 1613 cm^{-1} [25], dimethylacrylic acid displaying an absorption at 1600 cm^{-1} [26] or chain end vinyl produced in PBT photolysis at 1640 cm^{-1} [27]. It is noteworthy that:

- This absorbance appears as soon as the beginning of exposure.
- The absorbance ascribed to secondary alcohol decreases at the same time (see Fig. 5).

A possible explanation was the possibility of direct dehydration of isopropanol group [28]:

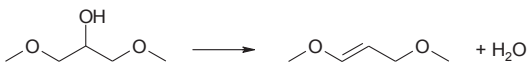

However, no spectral changes were observed in Vinyl Ester or in

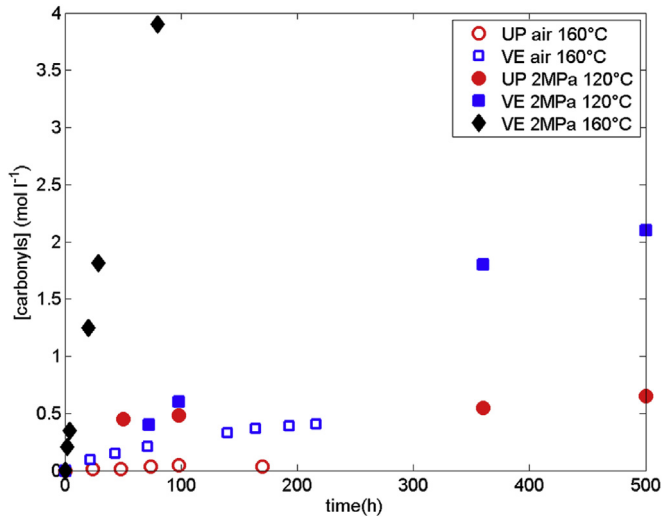

Fig. 7. Kinetic curves for carbonyl formation of UP and VE at several temperatures and under several oxygen pressures.

the material made of its prepolymer under vacuum (even after prolonged exposures).

Another possibility to explain that this dehydration reaction occurs only under oxidative condition is to consider that double bonds come from the reaction of alcohol with oxidation by products, as for example:

- The assisted dehydration of alcohol catalyzed by carboxylic acid groups,
- The crotonization of a hydroxyl carboxylic acids coming from the β scission reaction of alkoxy:

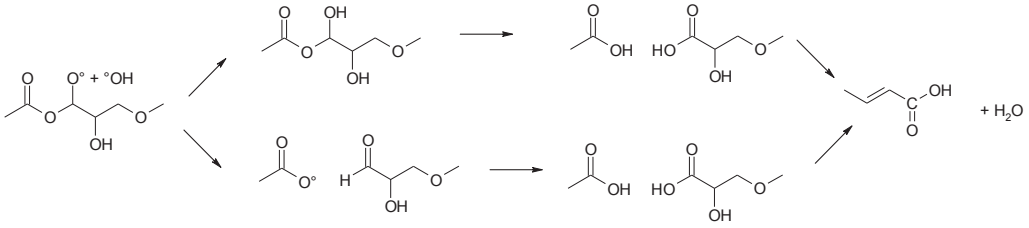

but the occurrence of this reaction remains to be proved.

4.2. On the position of reactive sites

Styrene cured unsaturated polyester and vinyl ester contains two kinds of oxidizable sites:

- The tertiary C–H in α position of aromatic rings of styrene.
- The secondary and tertiary C–H (belonging initially to the diol used for polyester synthesis) in α position of ester group.

According to the literature, styrenic units are expected to be very oxidizable, as for example illustrated:

- by the high proportion of benzaldehyde observed during the thermal oxidation at 350 °C monitored by GC-MS of an UP system close to the one under study [29].
- by the analysis of photo-oxidation products showing that styrene and polyester units are easily photo-oxidized [3].

However, the spectra in Fig. 6 showed that there is no evidence of characteristic products of styrenic units such as benzophenones: ~CH_2–CO–Ar at 1685 cm^{-1} [18]. Moreover, the main changes in FTIR spectra seem to be the same in VE and its prepolymer and in UP and its prepolymer (Fig. 6).

We will hence discuss on the nature of reactive sites by considering the kinetics of propagation i.e. the rate at which hydroperoxides are created. According to Korcek et al. [30], the rate constant of the reaction $POO^{\circ} + RH \rightarrow POOH + R^{\circ}$ is given by:

$$\log_{10} k_3^{s-POO^{\circ}}(30^{\circ}C) = 16.4 - 0.0525 \times BDE(C-H) \quad (1)$$

$$E_3 = 0.55 \times [BDE(C-H) - 261.5] \quad (2)$$

$$\log_{10} k_3^{t-POO^{\circ}}(30^{\circ}C) = 15.4 - 0.0525 \times BDE(C-H) \quad (3)$$

$$E_3 = 0.55 \times [BDE(C-H) - 272] \quad (4)$$

Where BDE(C–H) is the Bond Dissociation Energy of broken C–H.

- For cumene (representing styrenic units), literature [31] reports several values of rate constants ranging from 0.076 to 0.56 at 303 K and activation energies close to 40 kJ mol^{-1}. The estimation of k_3 at 160 °C ranges from 10 to 20 l mol^{-1} s^{-1}.
- For ethyl acetate (representing the CH_2 in α position of ester units), estimations of BDE by quantum calculations is reported to be stronger (ca 380–400 kJ mol^{-1}) [32,33]. The use of Eqs. (1)–(4) suggests that rate constant for propagation reaction on the –CO–O–CH_2– is on the same order of magnitude than for styrenic unit at 120–160 °C.

Moreover, the concentration in both sorts of C–H is:

- for styrenic units in both UP and VE: $[PH_{styrene}] \sim 1200/104 \times 0.3 = 4$ mol l^{-1}

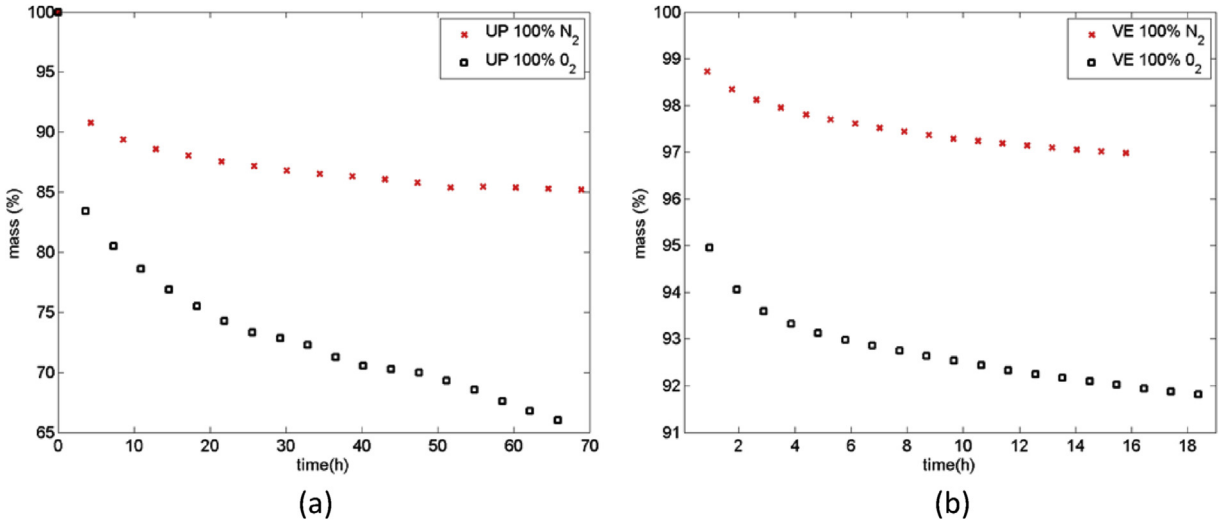

Fig. 8. Thermogravimetric analysis of unfilled UP and VE films (0.07 mm thickness) submitted to thermal a 160 °C ageing under 100% oxygen or nitrogen.

- for CH_2 in α position in UP: $[PH_{ester}] \sim 1200/156 \times 0.7 \times 2 = 11$ mol l^{-1}
- for CH_2 in α position in VE: $[PH_{ester}] \sim 4$ mol l^{-1} according to structure reported in Fig. 1.

In conclusion, propagation occurring on CH_2 in α position of ester is expected to be competitive with reactions on styrenic units for the ageing conditions under investigation.

Let's now turn to the stability of resulting hydroperoxides. On the assumption that hydroperoxides decompose mainly by an unimolecular process, it can be shown that the duration of induction period is given by:

$$t_i \sim 3/k_1 \quad (5)$$

Considering that oxidation kinetics of UP and VE do not display any induction period (Fig. 7), it means that k_1 is relatively high and that hydroperoxides involved in the thermal oxidative ageing of VE and UP are pretty unstable.

Cumene hydroperoxides stability is already documented [34,35]. Rate constant values (10^{-5} l mol^{-1} s^{-1} for bimolecular process and 10^{-5} s^{-1} for unimolecular process) suggest that even if some hydroperoxides are located on by styrenic unit, the characteristic time for their decomposition would be higher than the induction time for anhydride formation.

On the other hand, hydroperoxides located in α position of ester group are expected to be destabilized by electronic attractive effects. The rate constant for hydroperoxide decomposition was estimated ca 0.5 s^{-1} at 280 °C for PET [36]. The extrapolation of this value at 160 °C using any reasonable value for activation energy is clearly higher than the value of k_1 for POOH hold by styrenic units.

In conclusion, hydroperoxides are expected to be generated at a comparable rate on several reactive C—H. However, the hydroperoxides located in the vicinity of esters are pretty unstable and their

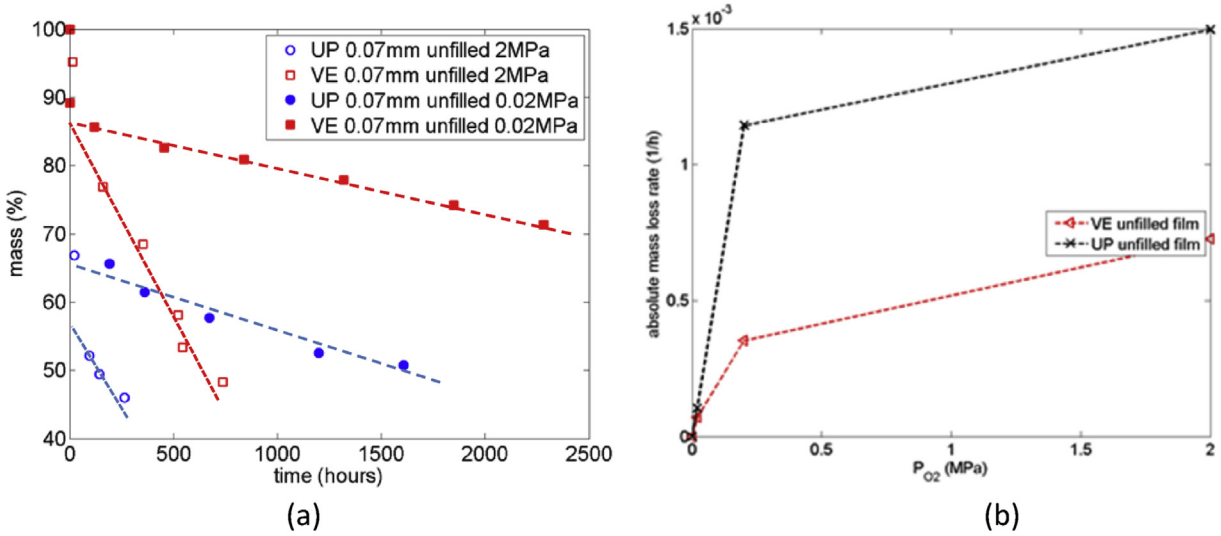

Fig. 9. Experimental mass loss of 70 μm thin films versus time for unfilled UP and VE samples aged at 160 °C under atmospherically air at 0.02 MPa or at 2 MPa (a) and effect of the oxygen pressure on the mass loss rate determined from the straight lines in Fig. 8a (b).

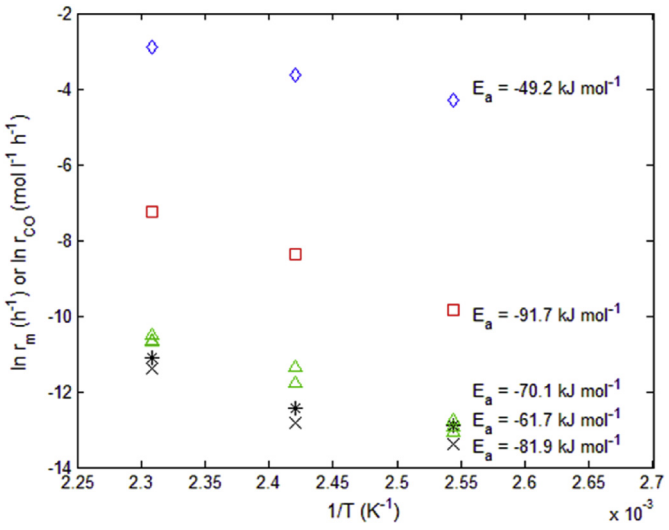

Fig. 10. Arrhenius diagram of degradation rate or mass loss rate for VE and VE composites: mass loss of 4 mm thick samples aged under air (×), mass loss of 2 mm thick samples aged under air (⁎), mass loss of 0.5 mm thick filled samples aged under 0.2 MPa O_2 (△), mass loss of 70 μm thick samples aged under 2.0 MPa (□), CO build up for 70 μm thick films aged under 2.0 MPa O_2 (◇).

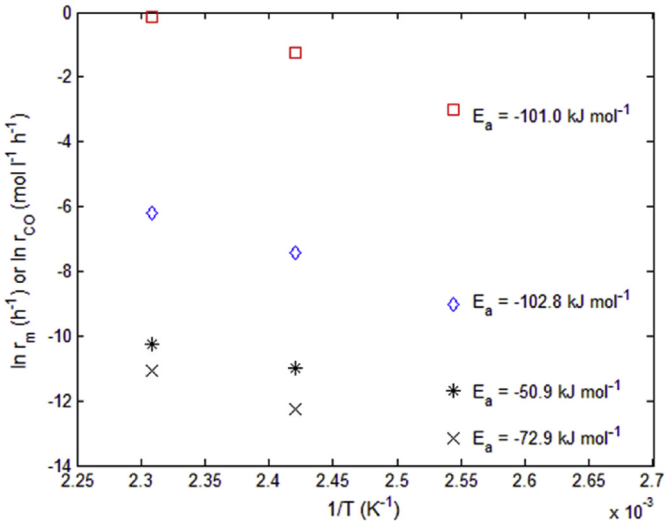

Fig. 11. Arrhenius diagram of degradation rate or mass loss rate for UP and UP composites: mass loss of 5 mm thick samples aged under air (×), mass loss of 2 mm thick filled samples aged under air (⁎), mass loss of 70 μm thick samples aged under 2.0 MPa (◇), CO build up for 70 μm thick films aged under 2.0 MPa O_2 (□).

fast decomposition explains the quasi instantaneous generation of anhydrides in both UP and VE.

4.3. On the differences in oxidative stability in UP and VE

The intrinsic oxidizability of ester sites are given by the rate of carbonyl build-up and mass loss under oxygen excess. They are respectively given by the ratio:

$$r_{CO} = \gamma_{CO}\frac{k^2_{3(POO^\circ+PH)}}{k_{6(POO^\circ+POO^\circ)}}\cdot[PH]^2 \tag{6}$$

$$r_m = \gamma_m\frac{k^2_{3(POO^\circ+PH)}}{k_{6(POO^\circ+POO^\circ)}}\cdot[PH]^2 \tag{7}$$

γ_{CO} and γ_m being the yields for carbonyl and volatile compounds formation from hydroperoxide decomposition.

① According to oxidation rate r_{CO} (Fig. 7), it is observed that Vinyl Esters are much more oxidizable than Unsaturated Polyesters. Since both polymers have the sort of same reactive site (CH_2 in α position of ester), it can be assumed that they have the same $k_{3(POO^\circ + PH)}$ value, and the same yield in anhydrides from hydroperoxide decomposition. Since the concentration in oxidizable sites is lower for VE than for UP (i.e. $[PH]_{VE} < [PH]_{UP}$), it means that the termination rate constant for $k_{6(POO^\circ + POO^\circ)}$ is higher for UP than for VE. It is clear that both materials under investigations are thermosets at glassy state and that T_g of Vinyl Ester is higher [37] than for Unsaturated Polyester [38], thus illustrating the possible link between the value of this termination rate constant and macromolecular mobility [39–41].

② It was seen that oxygen diffusion coefficient in UP and VE are very close in the investigated temperature range (Table 1), and that oxidation rate (r_{OX}, linked to the rate of carbonyl build-up) is higher for VE than for UP (Fig. 7). It is hence not surprising to witness that thickness of oxidized layers is lower for VE than for UP since [42]:

$$TOL \sim \sqrt{\frac{D_{O2}}{r_{OX}/[O_2]}} \tag{8}$$

③ Despite more intrinsically oxidizable, the mass loss rate for VE is lower than for UP. The simplest explanation is that materials differ by the volatile yield γ_m. The physical reason is that oxidation attacks randomly CH_2 in α position of ester sites. A volatile can be generated if two scissions occur on an elastically active chain (made of prepolymer) and generate a molecular product with a sufficiently low molar mass to allow its evaporation. From this point of view, volatile are more easily generated in UP where esters groups are separated by only 2 carbons atoms than in VE where they are located in chain ends.

④ The temperature dependence of oxidation kinetics was discussed by plotting rates of mass loss at steady state in an Arrhenius diagram for mass loss rate of thick samples aged under air, thin samples aged under enhanced oxygen pressure and some intermediary species (regarding the thickness or the oxygen pressure). Interpretation of data in Figs. 9 and 10 indicate that:

- for thin samples, the activation energy is linked to the activation energy of the mass loss induced oxidation process:

$(E_m)_{thin\ samples}$ ~ 100 kJ mol^{-1} for mass loss in UP.

$(E_m)_{thin\ samples}$ ~ 90 kJ mol^{-1} for mas loss in VE

- for thick samples, apparent activation energies for mass loss is significantly lower:

$(E_m)_{thick}$ ~ 50 kJ mol^{-1} for UP

$(E_m)_{thick}$ ~ 60–65 kJ mol^{-1} for VE

This decrease of activation energy when increasing the thickness would originate in the matter that mass loss kinetics are controlled by oxygen diffusion, the activation energy of which being lower than oxidation one (ca 30 kJ mol^{-1} vs 100 kJ mol^{-1}).

⑤ The comparison of activation energy for mass loss and carbonyl build-up for the oxidation of thin films exposed high oxygen pressure shows that:

E_{CO} ~ E_m ~ 100 kJ mol^{-1} for VE

E_{CO} ~ 50 kJ mol^{-1} for UP and E_m ~ 100 kJ mol^{-1}

According to Eq. (6) and Eq. (7):

$$E_{CO} = 2E_3 - E_6 + \phi_{CO} \quad (9)$$

$$E_m = 2E_3 - E_6 + \phi_m \quad (10)$$

ϕ_{CO} and ϕ_m expressing the temperature changes of yields in carbonyls and mass loss.

Two possible explanations can be proposed for the observed difference in UP:

- the high quantity of volatile compounds (Figs. 6 and 7) induces a possible underestimation of yield in carbonyl compounds (quantified by FTIR analysis in films) at high temperatures [43].
- the temperature dependence of changes of the yield of mass loss per initiation event, directly expressing the molar mass of the volatile products i.e., according to Eqs. (9) and (10), that $\phi_m > \phi_{CO}$ in UP and $\phi_m \sim \phi_{CO}$. Schematically, it would suggest that in UP, the increase with temperature of average molar mass of volatile compounds is stronger than for yield in carbonyl build-up. This explanation appears to be echoed in some previously published works [14,44,45] but remains speculative in the absence of quantification of VOC for isothermal ageing runs.

⑥ The fact that the temperature dependence for oxidation reactions (expressed by E_{CO}) is higher than for oxygen diffusion (see Table 1) suggests that the Thickness of Oxidized Layer decrease progressively when temperature is increased. This phenomenon would be less pronounced in UP (E_{CO} ~ 50 kJ mol^{-1}, E_D ~ 20 kJ mol^{-1}) than in VE (E_{CO} ~ 100 kJ mol^{-1}, E_D ~ 30 kJ mol^{-1}). This addresses the issue of extrapolating ageing data at lower temperature and the necessity to dispose of a robust kinetic model designed for reaction-diffusion coupling.

4.4. On the effect of fillers

Data in Table 1 show the oxygen diffusivity are very close for unfilled and filled materials. Moreover, based on thick samples mass loss experimental data, the calculation of the mass loss activation energy showed very close values (not shown) between the filled and unfilled samples.

It is surprising, at first sight, to observe that filler do not significantly influence the diffusion of oxygen in UP and VE. This behavior is surprising regarding the well documented cases of:

- semicrystalline polymers where crystals increase the barrier properties [46],
- nanofilled polymers as for example SiC particles in epoxy [47], silver particles in starch polymer [48],
- the effect of some metal oxides on the degradation at high temperature of some polyamides [49].

Sereda et al. [50] concluded that fillers lead to a decrease in oxygen diffusivity, provided that there is a good adhesion between polymer and filler, and particles are well dispersed and hinder the motions of polymer chain. This is not the case here, since the fillers particles clearly are of 10 μm diameter and Fig. 2 suggests that fillers are not sufficiently dispersed into the thermoset matrix. In other words, filers are not expected here to decrease the oxygen transport phenomena. Let us mention that this behavior permits to investigate the oxidation process for the filled materials only by knowing the fillers ratio and the unfilled material behavior and offers the possibility to elaborate the same kinetic model for filled and unfilled polymer.

5. Conclusions

The thermal oxidation of filled and unfilled films and plates of thermoset resins made of Vinyl Ester or Unsaturated Polyesters cured with styrene was studied at several temperatures and oxygen pressures. FTIR measurements showed the build-up of a carbonyl products which was concluded to be an anhydride coming from the oxidation of CH_2 in α position of the ester group. The kinetic curves for carbonyl formation showed that VE was more oxidizable than UP which was confirmed by the comparison of thickness of oxidized layers determined from optical microscopy and gravimetric data (ca 200 μm for VE vs 600 μm for UP aged at 160 °C under air according to optical microscopy). However, the yield of volatile compounds was observed to be greater for UP than VE which was discussed regarding the distance between oxidizable sites. From a practical point of view, it means that VE are intrinsically less stable than UP but will keep their neutron shielding performances longer than UP.

Acknowledgements

TN International is gratefully acknowledged for having granted this study.

Appendix. FTIR spectra of virgin resins

Basing on the existing literature [51,52] and classical FTIR tables, the absorption bands present in those spectra were assigned as follows (NB: it is intricate to interpret the fingerprint region for UP spectra, since it might be a combination of deformation C–O of ester groups and signal due to alcohol chain ends).

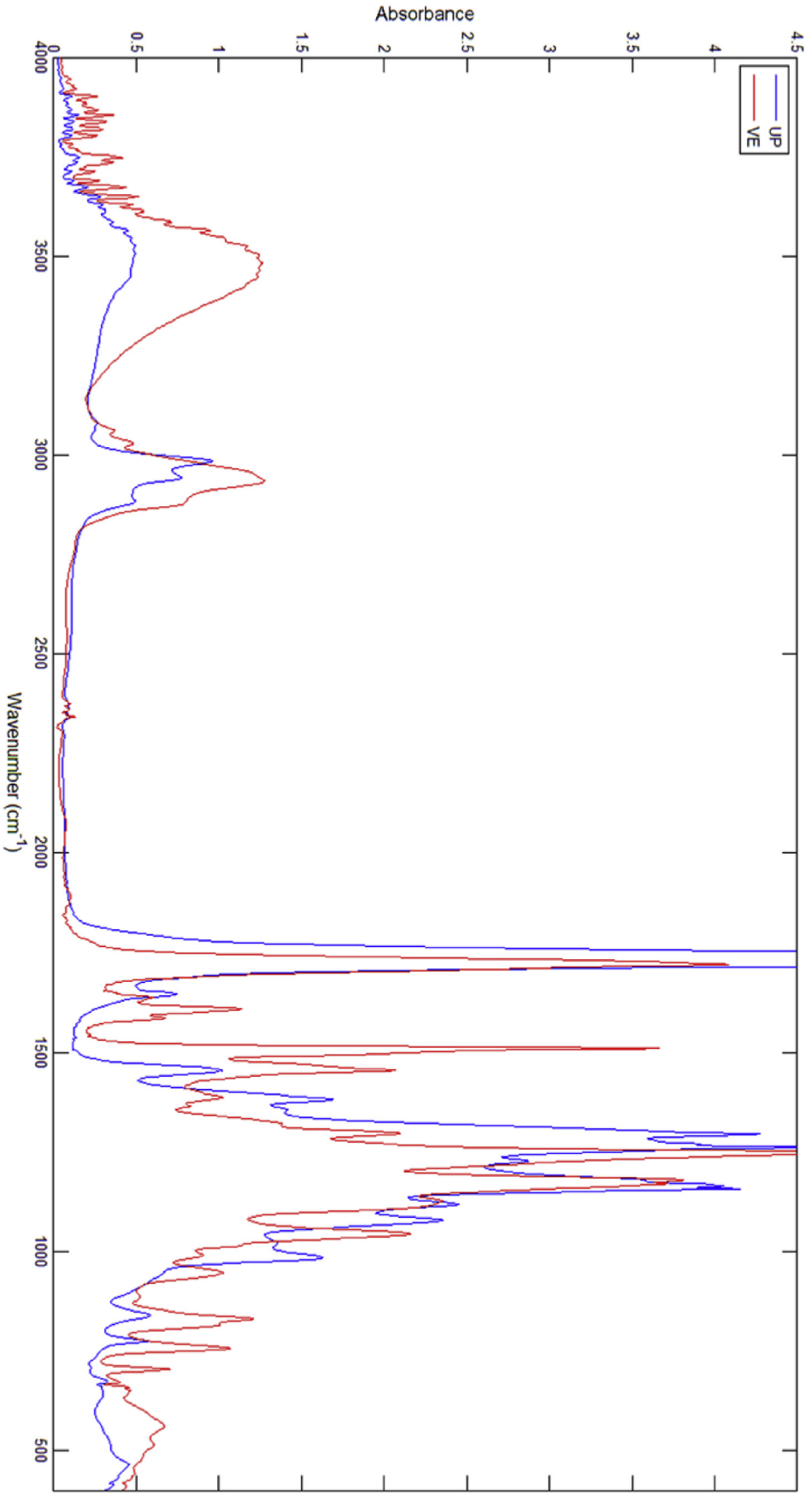

Fig. 12. FTIR spectra of virgin resins.

Table 2
FTIR absorption bands in UP. * observed in 1,2 propylene diol [53].

Wavenumber (cm^{-1})	Intensity	Functionnal group	Remark/type of vibration
3505	I or m, broad	ν(O−H)	stretching of prepolymer chain ends
3081	w	ν(aromatic C−H)	stretching
3064	w	ν(aromatic C−H)	stretching
2984	m	ν_d ($-CH_3$)	degenerate stretching
2943	m	ν_{as}(>CH_2) stretching	asymmetrical stretching
2883	m	ν_s(→C−H and >CH_2)	symmetrical stretching
1730	I	ν(>C═O ester)	stretching
1646	m	ν(>C═C<)	stretching
1454	m	δ_s(>CH−H)	in plane bending (scissoring)
1381	m	δ_S($-CH_3$)	symmetrical deformation (umbrella)
1355	w	δ($-CH_3$)	deformation
1295	I	ν(C−O ester)	Each sort of ester leads to a doublet
1262	I	ν(C−O carboxylic acids)	−CO−O−CH<
1228	m	ν(C−O alcohol) + δ(O−H)	−CO−O−CH_2−
1164	m		Chain ends carboxylic acids and alcohols have a fingerprint in the wavelength region as well
1157	m		
1119	m		
1079	m		
1021	w	ν(C−O ester)+ ν(C−O alcohol) + δ(O−H) + δ(−CH_2− styrene)	
985	m	δ(=C−H trans)	deformation
839	m	γ(−CH_2−CH(CH_3)-	skeletal vibration*
775	m	δ(styrenic C−H) oop	out of plane

Table 3
FTIR absorption bands in VE. *: a doublet at 990−950 cm^{-1} is observed in PMMA spectra [54].

Wavenumber (cm^{-1})	Intensity	Functionnal group	Remark/type of vibration
3460	I, broad	ν(O−H)	O−H stretch
3060	w	ν(aromatic C−H)	stretching
3028	w	ν(aromatic C−H)	stretching
2934	m	ν_a(>CH_2)	asymmetrical stretching
2895	m	ν_s(→C−H and −CH_2−)	symmetrical stretching
1720	I	ν(>C═O ester)	stretching
1637	m	ν(>C═C<)	stretching
1608	m	ν(>C═C< aromatic ring)	in-ring stretching
1585	m	ν(>C═C< aromatic ring)	in-ring stretching
1505	m	ν(>C═C< aromatic ring)	in-ring stretching
1455	m	δ_s(>CH_2) + δ_{as}(CH_3)	in-plane bending of >CH_2 (scissoring) + asymmetrical deformation of CH_3 (bending)
1385	w	δ_S($-CH_3$) + δ(>C(CH_3)$_2$)	bending
1295	m	δ(>CH−OH)	bending
1245	I	ν(Ar-O−CH_2− ether)	stretching
1180	m	ν(C−O ester)	stretching
1125	m	δ(>CH−OH) + δ(>CHO−H)	deformation
1045	w	δ(>CH−OH) + δ(>CHO−H)	deformation
990	w	δ(=C−H)	deformation of C−H in RCH═CH_2*
945	m	*	*
877	w	δ(styrenic C−H) oop	bending of ═C−H in 1,2 disubstituted aromatic (novolac)
830	m	δ(styrenic C−H) oop	bending of ═C−H in 1,4 disubstituted aromatic (epoxy vinyl ester)
757	m	δ(styrenic C−H) oop	bending of ═C−H in 1,2 disubstituted aromatic ═C−H (novolac)
703	m	δ(styrenic C−H) oop	bending of ═C−H in monosubstituted aromatic (styrene)

References

[1] Abadie P, Development of a new neutron shielding materials, TN™ resin VYAL for transport/storage casks for radioactive materials, 14th International Symposium on the Packaging and Transportation of Radioactive Materials (PATRAM 2004), Berlin, Germany, Paper No. 188.

[2] F. Bélan, V. Bellenger, B. Mortaigne, J. Verdu, Relationship between the structure and hydrolysis rate of unsaturated polyester prepolymers, Polym. Degrad. Stab. 56 (3) (1997) 301–309.

[3] S.Z. Jian, J. Lucki, J.F. Rabek, B. Ranby, Photooxidation and photostabilization of unsaturated crosslinked polyesters, ACS Symp. Ser. 280 (1985) 353–358.

[4] S. Michaille, P. Arlaud, J. Lemaire, Photolyse et photo-oxydation de polyesters insatures—1. Comportement du polymaleate de propylene glycol reticule ou non, Eur. Pol. J. 28 (3) (1992) 321–331.

[5] S. Michaille, P. Arlaud, J. Lemaire, Photolyse et photo-oxydation de polyesters insatures—2. Comportement du polymaleate-isophthalate de propylene glycol reticule ou non, Eur. Pol. J. 29 (1) (1993) 35–46.

[6] S. Michaille, P. Arlaud, J. Lemaire, Photolyse et photo-oxydation de polyesters insatures—3. comportement du poly(maleate orthophthalate) de propylene glycol, reticule ou non, Eur. Pol. J. 29 (8) (1993) 1053–1058.

[7] J. Sampers, E. Hutten, P. Gijsman, Accelerated weathering of unsaturated polyester resins. Aspects of appearance change, Polym. Test. 44 (2015) 208–223.

[8] A.W. Signor, M.R. VanLandingham, J.W. Chin, Effects of ultraviolet radiation exposure on vinyl ester resins: characterization of chemical, physical and mechanical damage, Polym. Degrad. Stab. 79 (2) (2003) 359–368.

[9] Y. Rodriguez-Mella, T. López-Morán, M.A. López-Quintela, M. Lazzari, Durability of an industrial epoxy vinyl ester resin used for the fabrication of a contemporary art sculpture, Polym. Degrad. Stab. 107 (2014) 277–284.

[10] A. Baudry, J. Dufay, N. Regnier, B. Mortaigne, Thermal degradation and fire behaviour of unsaturated polyester with chain ends modified by dicyclopentadiene, Polym. Degrad. Stab. 61 (3) (1998) 441–452.

[11] Y.F. Shih, R.J. Jeng, Thermal degradation behaviour and kinetic analysis of unsaturated polyester-based composites and IPNs by conventional and modulated thermogravimetric analysis, Polym. Degrad. Stab. 91 (4) (2006) 823–831.

[12] C. Joly, D. Le Cerf, C. Chappey, D. Langevin, G. Muller, Residual solvent effect on the permeation properties of fluorinated polyimide films, Sep. Purif. Technol. 16 (1) (1999) 47–54.

[13] D.W. Van Krevelen, K. te Nijenhuis, Properties of Polymers. Their Correlation with Chemical Structure; Their Structure Estimation and Prediction Additive Contribution, fourth ed., Amsterdam Elsevier, 2009, p. 655.

[14] J. Decelle, N. Huet, V. Bellenger, Oxidation shrinkage for thermally aged epoxy networks, Polym. Degrad. Stab. 81 (2) (2003) 239–248.

[15] X. Colin, C. Marais, J. Verdu, Kinetic modelling of the stabilizing effect of carbon fibres on thermal ageing of thermoset matrix composites, Comp. Sci. Technol. 65 (1) (2005) 117–217.

[16] X. Colin, C. Marais, J. Verdu, A new method for predicting the thermal oxidation of thermoset matrices: application to an amine crosslinked epoxy, Polym. Test. 20 (7) (2001) 795–803.

[17] C. Damian, E. Espuche, M. Escoubes, Influence of three ageing types (thermal oxidation, radiochemical and hydrolytic ageing) on the structure and gas transport properties of epoxy-amine networks, Polym. Degrad. Stab. 72 (3) (2001) 447–458.

[18] J. Rychly, L. Matisova-Rychla, K. Csmorova, L. Achimsky, L. Audouin, A. Tcharkhtchi, J. Verdu, Kinetics of mass changes in oxidation of polypropylene, Polym. Degrad. Stab. 58 (3) (1997) 269–274.

[19] J.L. Gardette, B. Mailhot, J. Lemaire, Photooxidation mechanisms of styrenic polymers, Polym. Degrad. Stab. 48 (3) (1995) 457–470.

[20] M. Gardette, S. Thérias, J. Gardette, M. Murariu, P. Dubois, Photooxidation of polylactide/calcium sulphate composites, Polym. Degrad. Stab. 96 (4) (2011) 616–623.

[21] E. Richaud, F. Farcas, P. Bartoloméo, B. Fayolle, L. Audouin, J. Verdu, Effect of oxygen pressure on the oxidation kinetics of unstabilised polypropylene, Polym. Degrad. Stab. 91 (2) (2006) 398–405.

[22] O. Okamba-Diogo, E. Richaud, J. Verdu, F. Fernagut, J. Guilment, B. Fayolle, Molecular and macromolecular structure changes in polyamide 11 during thermal oxidation, Polym. Degrad. Stab. 108 (2014) 123–132.

[23] A. Rivaton, Photochemistry of poly(butyleneterephthalate): 2—identification of the IR-absorbing photooxidation products, Polym. Degrad. Stab. 41 (3) (1993) 297–310.

[24] N. Longiéras, M. Sebban, P. Palmas, A. Rivaton, J.L. Gardette, Degradation of epoxy resins under high energy electron beam irradiation: radio-oxidation, Polym. Degrad. Stab. 92 (12) (2007) 2190–2197.

[25] Y. Mikawa, Characteristic absorption bands of vinyl ethers, Bull. Chem. Soc. Jpn. 29 (1) (1956) 110–115.

[26] http://www.sigmaaldrich.com/catalog/product/aldrich/d138606?lang=fr&region=FR.

[27] A. Rivaton, Photochemistry of poly(butyleneterephthalate): 1—identification of the IR-absorbing photolysis products, Polym. Degrad. Stab. 41 (3) (1993) 283–296.

[28] N. Grassie, M.I. Guy, N.H. Tennent, Degradation of epoxy polymers: part 4—thermal degradation of bisphenol-A diglycidyl ether cured with ethylene diamine, Polym. Degrad. Stab. 14 (2) (1956) 125–137.

[29] A. Baudry, J. Dufay, N. Regnier, B. Mortaigne, Thermal degradation and fire behaviour of unsaturated polyester with chain ends modified by dicyclopentadiene, Polym. Degrad. Stab. 61 (3) (1998) 441–452.

[30] S. Korcek, J.H.B. Chenier, J.A. Howard, K.U. Ingold, Absolute rate constants for hydrocarbon autoxidation, Can. J. Chem. 50 (14) (1972) 2285–2297.

[31] E.T. Denisov, I.B. Afanas'ev, Oxidation and Antioxidants in Organic Chemistry and Biology, CBC Taylor & Francis Group, Boca Raton/London/New York/Singapore, 2005, p. 47.

[32] V. Saheb, S. Mohammad, A. Hosseini, Theoretical studies on the kinetics and mechanism of multi-channel gas-phase unimolecular reaction of ethyl acetate, Comput. Theor. Chem. 1009 (2013) 43–49.

[33] B. Akih-Kumgeh, J.M. Bergthorson, Structure-reactivity trends of C1–C4 alkanoic acid methyl esters, Combust. Flame 158 (6) (2011) 1037–1048.

[34] http://www.sigmaaldrich.com/catalog/product/aldrich/247502?lang=fr&region=FR.

[35] E.T. Denisov, I.B. Afanas'ev, Oxidation and Antioxidants in Organic Chemistry and Biology, CBC Taylor & Francis Group, Boca Raton/London/New York/Singapore, 2005, p. 185 (Table 4.12).

[36] L.K. Nait-Ali, X. Colin, A. Bergeret, Kinetic analysis and modelling of PET macromolecular changes during its mechanical recycling by extrusion, Polym. Degrad. Stab. 96 (2) (2011) 236–246.

[37] T.F. Scott, W.D. Cook, J.S. Forsythe, Kinetics and network structure of thermally cured vinyl ester resins, Eur. Pol. J. 38 (4) (2002) 705–716.

[38] N. Taheri Qazvini, N. Mohammadi, Dynamic mechanical analysis of segmental relaxation in unsaturated polyester resin networks: effect of styrene content, Polymer 46 (21) (2005) 9088–9096.

[39] E. Richaud, P.Y. Le Gac, J. Verdu, Thermooxidative aging of polydicyclopentadiene in glassy state, Polym. Degrad. Stab. 102 (2014) 95–104.

[40] T. Devanne, A. Bry, N. Raguin, M. Sebban, P. Palmas, L. Audouin, J. Verdu, Radiochemical ageing of an amine cured epoxy network. Part II: kinetic modelling, Polymer 46 (1) (2005) 237–241.

[41] S. Shimada, Y. Hori, H. Kashiwabara, Relation between diffusion controlled decay of radicals and α-relaxation in polyethylene and polyoxymethylene, Polymer 22 (10) (1981) 1377–1384.

[42] L. Audouin, V. Langlois, J. Verdu, J.C.M. de Bruijn, Role of oxygen diffusion in polymer ageing: kinetic and mechanical aspects, J. Mater. Sci. 29 (3) (1994) 569–583.

[43] A. François-Heude, E. Richaud, J. Leprovost, M. Heninger, H. Mestdagh, E. Desnoux, X. Colin, Real-time quantitative analysis of volatile products generated during solid-state polypropylene thermal oxidation, Polym. Test. 32 (5) (2013) 907–917.

[44] X. Colin, C. Marais, J. Verdu, Kinetic modelling and simulation of gravimetric curves: application to the oxidation of bismaleimide and epoxy resins, Polym. Degrad. Stab. 78 (3) (2002) 545–553.

[45] V. Bellenger, J. Decelle, N. Huet, Ageing of a carbon epoxy composite for aeronautic applications, Comp. B Eng. 36 (3) (2005) 189–194.

[46] V. Compañ, L.F. Del Castillo, S.F. Hernández, M. Mar López-González, E. Riande, Crystallinity effect on the gas transport in semicrystalline coextruded films based on linear low density polyethylene, J. Polym. Sci. B Polym. Phys. 48 (6) (2010) 634–642.

[47] H. Alamri, I.M. Low, Effect of water absorption on the mechanical properties of nano-filler reinforced epoxy nanocomposites, Mater. Des. 42 (2012) 214–222.

[48] P. Cheviron, F. Gouanvé, E. Espuche, Starch/silver nanocomposite: effect of thermal treatment temperature on the morphology, oxygen and water transport properties, Carbohydr. Polym. 134 (10) (2015) 635–645.

[49] E. Duemichen, U. Braun, H. Sturm, R. Kraemer, P. Deglmann, S. Gaan, R. Senz, A new molecular understanding of the thermal degradation of PA 66 doped with metal oxides: experiment and computation, Polym. Degrad. Stab. 120 (2015) 340–356.

[50] L. Sereda, M. Mar López-González, L.L. Yuan Visconte, R.C.R. Nunes, R. Russi Guimarães Furtado, E. Riande, Influence of silica and black rice husk ash fillers on the diffusivity and solubility of gases in silicone rubbers, Polymer 44 (10) (2003) 3085–3093.

[51] M. González González, J.C. Cabanelas, J. Baselga, in: Theophile Theophanides (Ed.), Applications of FTIR on Epoxy Resins - Identification, Monitoring the Curing Process, Phase Separation and Water Uptake, Infrared Spectroscopy – Materials Science, Engineering and Technology, 2012. ISBN: 978-953-51-0537-4, InTech, Available from: http://www.intechopen.com/books/infrared-spectroscopymaterials-science-engineering-and-technology/applications-of-ftir-on-epoxy-resins-identification-monitoringthe-curing-process-phase-separation.

[52] G. Nikolic, S. Zlatkovic, M. Cakic, S. Cakic, C. Lacnjevac, Z. Rajic, Fast Fourier transform IR characterization of epoxy GY systems crosslinked with aliphatic and cycloaliphatic polyamine adducts, Sensors 10 (2010) 684–696.

[53] http://www.fao.org/docrep/w6355e/w6355e0t.htm.

[54] L. Yingshua, H. Weihua, L. Zhisong, M.L. Chang, Photografted poly(methyl methacrylate)-based high performance protein microarray for hepatitis B virus biomarker detection in human serum, Med. Chem. Commun. 1 (2010) 132–135.